Contrail minimization through altitude diversions

A feasibility study leveraging global data

Roosenbrand, Esther; Sun, Junzi; Hoekstra, Jacco

Contents lists available at ScienceDirect

Transportation Research Interdisciplinary Perspectives

journal homepage: www.elsevier.com/locate/trip

Contrail minimization through altitude diversions: A feasibility study leveraging global data

Esther Roosenbrand *, Junzi Sun, Jacco Hoekstra

Faculty of Aerospace Engineering, Delft University of Technology, Kluyverweg 1, 2629 HS, Delft, The Netherlands

ARTICLE INFO

ABSTRACT

As global flight volume rises, the aviation industry is facing increasing climate challenges. One major factor is the impact of contrails, which trap outgoing terrestrial radiation and counteract emission reduction benefits from emission-optimized flight routes. Our study quantifies contrail-forming flights globally and assesses altitude adjustments necessary to avoid these regions. Using the Integrated Global Radiosonde Archive and global flight data from 2021-2022, we highlight several contrail-prone regions with high air traffic volumes and high potential for contrail-formation. We propose an operational strategy in altitude diversion, which can halve the amount of persistent contrails. Further, we analyse the additional carbon emissions caused by the altitude diversions and safety risks in terms of potential new conflicts. Our findings provide actionable strategies for policymakers to balance climate mitigation and operational challenges in aviation.

1. Introduction

Global aviation currently accounts for approximately 5% of net anthropogenic climate forcing (Lee, 2021), and this contribution is expected to increase as air traffic continues to rise worldwide. As a result, sustainability has become one of the most pressing challenges facing the aerospace industry. While alternative fuels and aerodynamic aircraft hold promise for reducing emissions, their implementation on a commercially relevant scale is still years away.

In addition to carbon dioxide, aircraft emissions also include nitrogen oxides, water vapour, sulphur oxides, and aerosols (Lee et al., 2010). However, the most significant individual contributor to aviation's total radiative forcing at shorter timescale is the formation of contrail cirrus, albeit with some uncertainties (Grewe et al., 2017). While carbon dioxide emitted today impacts global warming within 20–40 years, the warming effect of contrails is immediate (Avila et al., 2019).

This emphasizes the importance of minimizing contrails as a way to limit aviation's climate impact immediately as well as into the future. To address this challenge, the novel application of multidisciplinary fields beyond aviation, such as combining global aircraft surveillance data, atmospheric science, and satellite remote sensing, can help create a climate-optimized trajectory generator.

This paper aims to quantify the global extent of contrail-forming flights, their geographical location, as well as the typical altitude deviation necessary to avoid contrail-forming regions. Research done in Teoh et al. (2022), utilizes ERA5 reanalysis from ECMWF and an air traffic dataset from NATS (UK air navigation). Investigating the feasibility of incremental step-wise altitude diversion has been researched in Avila et al. (2019) in accordance with Domestic Reduced Vertical Separation Minimum (DRVSM) rules, using a year's worth of NOAA's Rapid Refresh Products (RAP) and a repeatedly using a single day of ADS-B data of mainland USA (24,095 flights).

This paper uses weather balloon data from the open-source Integrated Global Radiosonde Archive, as in Agarwal et al. (2022), where the radiosondes were used to validate reanalyses data like ECMWF and MERRA-2 to determine the estimation accuracy of contrail formation.

Additionally, the potential climate gain of these deviated flights will be computed in terms of radiative forcing (RF), applying the same net radiative forcing model as in Avila et al. (2019). Similar to the approach used in Rosenow and Fricke (2019), where the radiative forcing of individual condensation trails was calculated. Regarding the additional emissions caused by altitude changes, in previous research this was calculated using BADA, a database of Aircraft from EUROCONTROL (Teoh et al., 2022). This combination provides a sense of the overall true climate impact of altitude deviations to prevent contrails.

Furthermore, the potential safety impacts of contrail-mitigation are investigated. Through work has been done on this topic in Simorgh et al. (2023), which utilizes scenarios with around 1,000 flights during a 4-hour time frame in the Spanish and Portuguese airspace. Similarly, in Sausen et al. (2023), 212 aircraft were deviated vertically in MUAC airspace in order to avoid contrail formation.

---

* Corresponding author.
E-mail addresses: e.j.roosenbrand@tudelft.nl (E. Roosenbrand), j.sun-1@tudleft.nl (J. Sun), j.m.hoekstra@tudelft.nl (J. Hoekstra).
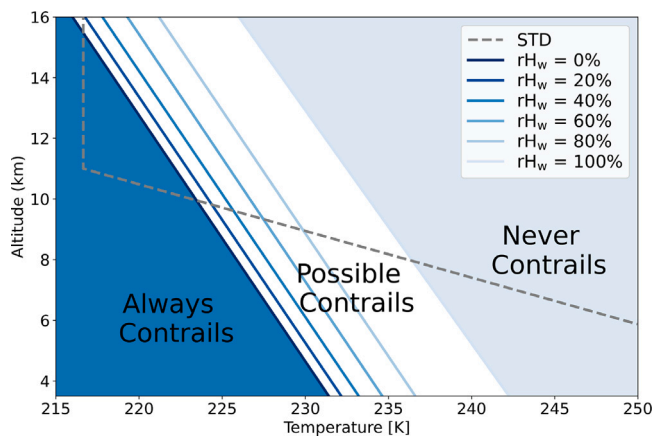
Fig. 1. A Schmidt-Appleman Diagram where the solid lines indicate the threshold temperatures at 0, 20, 40, 60, 80 and 100% relative humidity respectively, for kerosene fuel and an overall propulsion efficiency of 0.4. The international standard atmosphere temperature profile (STD) is plotted as well.

Our paper utilizes over 5.7 million flights, 2 years of real world data with global coverage, focusing on altitude changes rather than changing latitudinal or longitudinal positions. The assumption is that the flights are already horizontally and vertically separated according to safety protocols. We also solely consider the feasibility of altitude changes at the tactical short-term decisions, not possible strategical or pre-tactical decisions. Recent work regarding this has been done by Baneshi et al. (2023) and Simorgh et al. (2022).

By utilizing new data sets, this paper provides an alternate geographic coverage, as well as utilizing the high vertical resolution for the altitude deviation.

2. Contrails

2.1. Theories for contrail formation

Contrails, resembling clouds, can emerge in the wake of aircraft. To initiate contrail formation, certain atmospheric conditions must be met: the air temperature should be below −40 °C (233.15 K), and there should be a high relative humidity (Schumann, 1996). The formation of contrails is determined by the Schmidt–Appleman criterion (SAC) (Schumann et al., 2011), a thermodynamic theory developed by Schmidt and Appleman, which was later revised by Schumann (1996). The SAC states that the formation of contrails from condensing exhaust water depends on ambient pressure, humidity, and the ratio of water and heat released into the exhaust plume. When an aircraft flies through atmospheric conditions that satisfy the SAC, saturation with respect to liquid water occurs, resulting in contrail formation.

Fig. 1 shows the Schmidt-Appleman Diagram, which can be divided into three sections: always contrails, possible contrails, and never contrails. If the ambient temperature exceeds the line of relative humidity with respect to water (RH_w) at 100%, contrails are not expected to form (Service, 1981; Schumann, 2005). In conditions where the ambient temperature falls below the relative humidity line of 0%, contrails should always form. When the point lies between these two lines, in the *possible contrail* section of the graph, the formation of contrails depends on the relative humidity at that point, determining whether it falls on the left (always contrail) or right (never contrail) side of the corresponding RH_w line.

2.2. Climate impact contrails

While many contrails disappear quickly, persistent contrails have lifetimes of more than five minutes, occurring when the condensing exhaust water does not evaporate in that given time frame (Ferris, 2007). Persistent contrails contribute to global warming by trapping outgoing terrestrial radiation (Schumann, 1996). This creates an imbalance between the incoming solar radiation and radiation from the Earth's atmosphere and surface, causing radiative forcing (RF) which leads to an alteration of temperature in the lower atmosphere (Karcher, 2018).

Whether a contrail is persistent is indicated by the presence of an ice-supersaturation region (ISSR), which forms when the ambient air is supersaturated with respect to ice (Schumann, 1996). Therefore, for persistent contrail formation, the aircraft must fly through a part of the atmosphere that satisfies both the SAC (indicating contrails can theoretically form) and is an ISSR (indicating their persistence).

Although contrails have a warming impact on global climate by trapping outgoing radiation, the impact of daytime contrails can be counteracted by their cooling impact, making their overall effect uncertain (Schumann et al., 2011). Nighttime contrails, however, always have a warming impact. Analysis from Stuber et al. (2006) showed that while night flights account for only 25 percent of air traffic, they account for 60 to 80 percent of the contrail climate forcing. Similarly, while winter flights are 22 percent of annual air traffic, they contribute to half of the annual mean forcing (Stuber et al., 2006). This paper includes a day and nighttime analysis, as well as seasonal variations, to more specifically understand the contribution of contrails to global climate change.

2.3. Contrail detection and avoidance

In practice, avoiding persistent contrail-forming atmospheric regions often involves either flying around the perimeter or changing altitude (Avila et al., 2019). The expansiveness of these regions typically makes re-routing less environmentally effective than varying altitude (Gao and Hansman, 2013; Sridhar et al., 2014). This implies that contrail avoidance would need to be incorporated into the flight planning process.

The deviations need to be in accordance with Domestic Reduced Vertical Separation Minimum (DRVSM) rules (Avila et al., 2019). Before such climate-optimized routing can be implemented, contrail formation needs to be adequately predicted, for re-routing but also for developing metrics to enforce compliance from airlines and industry.

3. Data

The assessment of the number of flights that fall within a persistent contrail-forming atmospheric region and the required altitude change to leave the region, are based on remote sensing and flight data. This section explains these data sources and the steps taken before further processing.

3.1. Integrated global radiosonde archive

The Integrated Global Radiosonde Archive (IGRA) consists of radiosonde observations collected and maintained by the US National Centers for Environmental Information (NCEI) of the US National Oceanic and Atmospheric Administration (NOAA) (Durre et al., 2018). Radiosondes are launched once or twice daily, usually at 0000 and 1200 UTC. During the 1 to 2-hour ascent, the radiosonde instruments collect measurements that are transmitted to ground stations (Durre et al., 2021).

At the ground station, the data is processed into pressure, geopotential height, temperature, and derived wind direction and speed based on the latitude and longitude of the balloon. In some cases, relative humidity with respect to water (RH_w) is also measured. For assessing persistent contrail formation, relative humidity with respect to ice is a crucial parameter, as any value of RH_w exceeding 100% indicates the presence of an ISSR. While $RH_w > 100\%$ does not occur in the Earth's
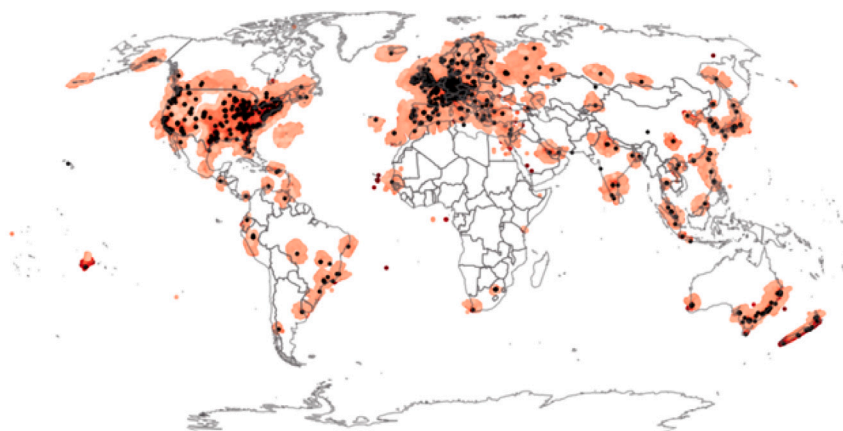
(a) OpenSky receiver locations and coverage in 2022 (sourced from: Sun et al. (2022)).
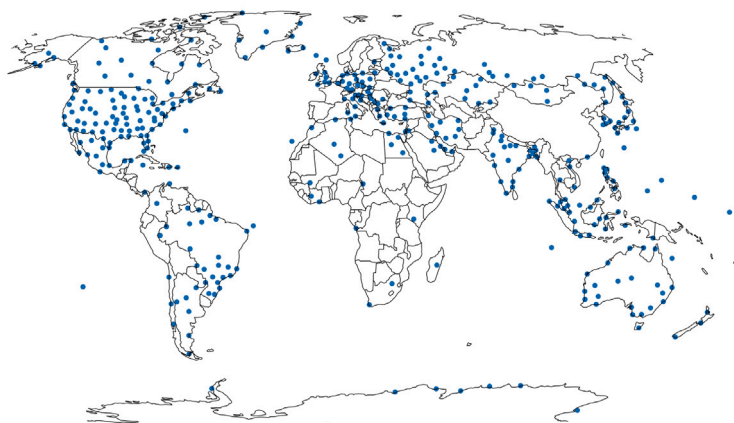
(b) IGRA station locations used in this research

Fig. 2. Research Area: the OpenSky receiver locations and the IGRA stations that have an OpenSky receiver nearby.

atmosphere, relative humidity with respect to ice, RH_i, exceeding 100% is one of the criteria for persistent contrails and is common (Sonntag, 1994).

There are several ways of determining the RH_i based on the RH_w. In this study, we use the formulas (Eqs. (1) and (2)) developed by Sonntag (1994). The equilibrium vapour pressure of water molecules (e_w) or ice (e_i) is temperature-dependent and can be used to determine the relative humidity with respect to water and ice (Buehler and Courcoux, 2003).

$$RH_w = \frac{e}{e_w} \tag{1}$$

$$RH_i = \frac{e}{e_i} \tag{2}$$

Previous research (Soden and Lanzante, 1996; Moradi et al., 2010) shows good agreement between IGRA relative humidity measurements and satellite data, with mean differences of 1 to 3%. The IGRA sensors (such as the Vaisala RS92) themselves have been shown to have an accuracy within ± 1 K for temperature (Dirksen et al., 2014) and 10% for the relative humidity (Miloshevich et al., 2009).

3.2. Flight data: OpenSky and Spire

To ensure global coverage, two flight data sources were used in this research: OpenSky and Spire. The OpenSky Network, which has been collecting global air traffic surveillance data since 2013, provides unfiltered and raw data based on ADS-B, Mode S, TCAS, and FLARM messages that are open for use (Strohmeier et al., 2021). The spatial coverage is visualized in Fig. 2.a, with black dots representing station

locations and red shading indicating the coverage of each station. The coverage is highest over Europe and North America, whereas due to the nature of terrestrial ADS-B, coverage over the oceans is minimal.

On the other hand, Spire uses satellite in addition to ground receivers, enabling ocean coverage. Since July 2018, a constellation of hundreds has been collecting ADS-B data globally. While OpenSky provides year-round temporal coverage, Spire data is available to us only for the month of April.

4. Method

In this section, we outline the methodology used to quantify the number of flights that fall within persistent contrail-forming atmospheric regions and the necessary altitude change required to leave these regions.

4.1. Contrail quantification

Unfortunately, only 304 of the 695 station locations measure the parameter of relative humidity over water vapour, which is necessary to determine the relative humidity over ice.

To identify flights that fall within ISSRs, we draw a 100×100 km^2 square around each IGRA station location. This area is deemed to be a representative area of influence for a single IGRA measurement, considering the lateral expansive nature of ISSR (Avila et al., 2019). We then overlay the locations of OpenSky receivers with these polygons.

If an OpenSky receiver is located within an IGRA polygon, we use the corresponding IGRA measurement location and OpenSky receiver data in our research. For cases where there is no OpenSky receiver
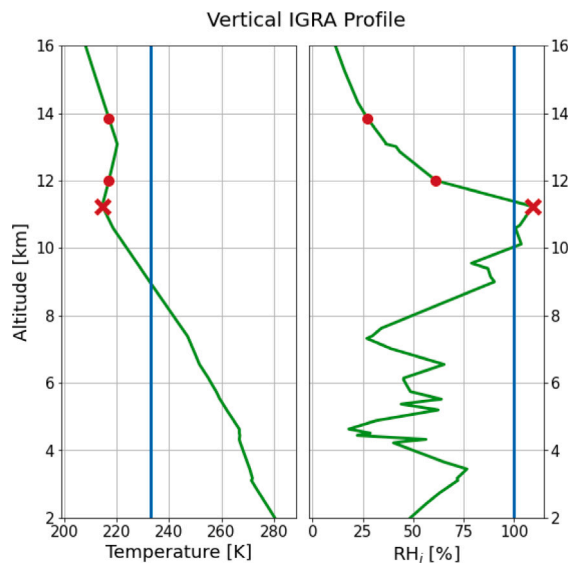
Fig. 3. An example of a vertical profile of temperature (left) and relative humidity (right) w.r.t. ice at the Camborne, a U.K. station on December 12, 2022 only. One of the aircraft is indicated in both plots by a cross (here at an altitude of 11.2 km) satisfies both SAC and the ISSR criterion, thus produces persistent contrails. The two aircraft at higher altitudes (indicated by dots) satisfy SAC but not the ISSR criterion, thus should produce non-persistent contrails.

within the IGRA polygon, we use Spire flight data. This data intersection results in coverage of 72 countries, the locations of the stations are shown as black dots in Fig. 10.

Only aircraft at cruise are considered, and the flight altitude closest to the weather balloon station (at the centre of each polygon) is used. Using this flight data, we then calculate the number of flights that pass through each polygon and identify those that fall within persistent contrail-forming atmospheric regions.

4.2. Flight level change

In Fig. 3, we present an example of a vertical profile of temperature and relative humidity with respect to ice for the Camborne station (UK) on December 12, 2022. The temperature profile on the left shows the vertical blue line indicating the −40 °C (233.15 K) SAC condition for contrail formation. On the right, the 100% RH_i is shown as a blue line, representing the ice-supersaturation condition.

Moreover, the figure also includes the representation of aircraft at their respective flight levels along with the vertical relative humidity profile. A cross in both plots indicates one of the aircraft located at an altitude of 11.2 km satisfying both the SAC and ISSR criteria, thereby producing persistent contrails.

In Fig. 3, it is also demonstrated that a small increase in altitude, only a few hundred feet, could cause the aircraft indicated by a cross to descend below the 100% RH_i line, thereby ceasing to satisfy the ISSR condition and stop producing persistent contrails.

Flight level changes that would exceed FL400 are not included in this analysis.

4.3. Net radiative forcing

As explained in Section 1, the foremost climate impact of contrails is through their trapped radiative forcing. Radiative forcing (RF) is a measure of the contribution of a greenhouse gas to the radiative energy budget of the climate system on Earth, which can disrupt the balance of incoming and outgoing energy in the atmosphere and alter the eQuilibrium state of the climate system (Ramaswamy et al., 2001). Measuring this impact can be done through net radiative forcing, which

is the sum of incoming solar shortwave radiation (RF_{SW}) and outgoing longwave radiation (RF_{LW}).

Shortwave radiation from the sun is scattered or reflected by clouds and aerosols, or absorbed in the atmosphere (Trenberth et al., 2009; Sanz-Morère I. Eastham et al., 2021). On the other hand, longwave or terrestrial radiation refers to the infrared radiation emitted by the Earth, which is absorbed by clouds before being re-emitted. Contrails, similar to natural cirrus clouds, reflect incoming solar radiation during the daytime, resulting in a negative shortwave radiation effect. However, they also absorb terrestrial radiation and re-emit it at a higher altitude, leading to a positive longwave radiation effect during both day and night (Sanz-Morère I. Eastham et al., 2021).

To quantify the radiative effects of contrails, we will use the cloud radiative-transfer model (Corti and Peter, 2009). This model calculates the contrail-induced radiative imbalance in net warming of the Earth (Sanz-Morère I. Eastham et al., 2020). A positive RF_{Net} would indicate an increase in the net energy of the Earth-atmosphere system.

4.4. Additional fuel burn

The additional fuel burn required for the altitude manoeuvres was determined using OpenAP (Sun et al., 2020), which is an open-source aircraft performance model capable of estimating fuel consumption and emissions based on flight data.

Based on the necessary altitude change, the additional fuel burn is determined, based on the aircraft type, altitude, vertical rate, and speed. A sensitivity analysis is performed on the initial mass parameter (0.70, 0.85, and 0.90% of the maximum take-off weight). The type code and engine parameters are based on the ICAO 24-bit transponder code, an aircraft identifier gathered from the ADS-B data. From this fuel flow analysis, the additional CO_2 emissions can be derived.

4.5. Risks to separation from altitude changes

Uncoordinated flight changes cannot always be safely performed. In Figs. 4, two scenarios illustrate the potential risks to separation caused by altitude changes to avoid contrail-forming areas. The sole criterion for an altitude diversion is that it is the shortest vertical way out, and the absolute change is less than 2000 ft.

Even though a loss of separation does not always imply an impending collision, it does signify aircraft being closer than safety regulations. A loss of separation occurs when aircraft within distance less than 5 nautical miles (9.26 km) and less than 1000 ft (300 m) altitude difference. A conflict is a predicted loss of separation, and uses the protected aircraft zone (Organization, 2016).

In this study, we determine nearby aircraft using a kd-tree algorithm. The *cKDTree* library from the *scipy* Python package is used as an efficient way to perform such calculations. We first search for 10 nearest aircraft for each individual aircraft, then the ones with distances below 5 nm are selected. Subsequently, these are also filtered with a maximum vertical distance of 1000 ft.

The loss of separation detection is first performed with the ADS-B data from OpenSky with the original altitude and then with the data including altitude diversions. This allows for the identification of intrusions similar to those sketched in Fig. 4.b.

Besides this intermediate loss of separation, Fig. 4.a shows a future conflict. Based on the track and ground speed from the ADS-B data, an extrapolation was made for the trajectories for a look-ahead time of 10 min. It was investigated whether the extrapolated trajectories of the five nearest neighbours intersected. If so, this intersection was treated as a conflict.

5. Results

In this section, we evaluate the results and discussion, subdividing our analysis into several parts:
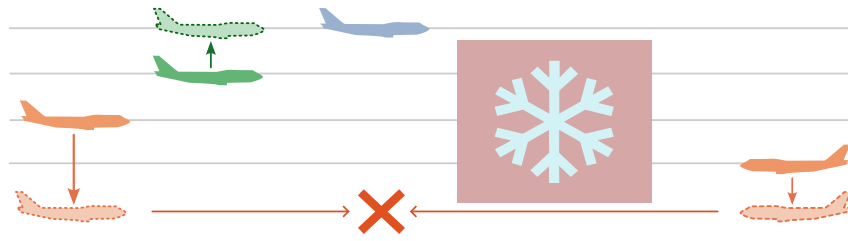
(a) Example of a conflict. The red box with a snowflake indicates a contrail-forming region that should be avoided. The blue aircraft does not have to change its altitude, and the green aircraft needs to increase its altitude. The orange aircraft both need to decrease their altitudes, and thus creating a conflict.
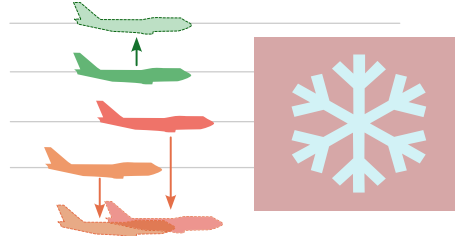

(b) Example of a potential loss of separation. The green aircraft increases its altitude to avoid the contrail-forming area without difficulties. The two orange aircraft are initially vertically separated, but because they both decrease their altitude, a loss of separation occurs.

Fig. 4. Two scenarios illustrating the potential risks to separation caused by altitude changes to avoid contrail-forming areas.
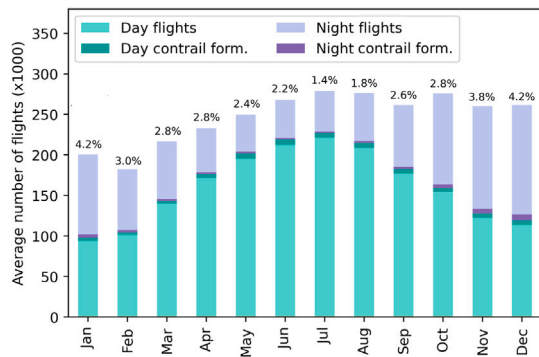
(a) Average number of flights per month in 2021 and 2022 in our dataset, with colours indicating day or nighttime flights, and whether they create contrails (indicated by the percentage above the bars).
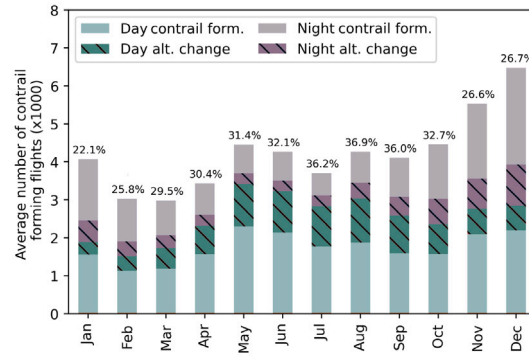
(b) Average number of contrail-forming flights in 2021 and 2022 in our dataset and the subset of flights that are suitable for an altitude change of less than 2000 ft, indicated by hatching (indicated by the percentage above the bars).

Fig. 5. Temporal effects of contrail formation.

5.1. Quantifying contrails

Following the method described in Section 4, we analysed a total of 5,722,588 flights. Of these, 202,240 (3.5%) were identified as satisfying both the SAC and ISSR conditions, indicating the production of persistent contrails.

5.2. Temporal effects

As described in Section 1, seasonality has a large impact on contrail formation. In addition, the time of day when contrails form influences the climate impact. We consider these two temporal effects in this subsection.

In Fig. 5.a, we show the total number of flights per month, with colours indicating day and nighttime flights, as well as the percentage of total flights that create contrails (percentage above the bars). These values represent the monthly averages from 2021 and 2022. While air traffic peaks in the (Northern Hemisphere's) summer months, there is

a higher occurrence of persistent contrails during winter, according to Avila et al. (2019). In Fig. 5.a, we observe a similar result. Although the total number of flights is lowest during the winter months, the number of days with persistent contrail-forming atmospheric conditions and the percentage of contrail-producing flights per month peak during the winter months. Since the IGRA sounding data is global, with 87% of the stations located in the Northern Hemisphere (as seen in Fig. 2), we apply the Northern Hemisphere seasonal cycle to our analysis.

Fig. 5.b shows the number of contrail-forming flights, with colours indicating day or night, and hatching indicating the portion where an altitude change of less than 2000 ft would stop contrail formation.

5.3. Geographical effects

In addition to the temporal effects discussed in the previous section, contrail formation is also expected to vary based on geographical location. By utilizing the global nature of the OpenSky, Spire, and IGRA data, we examine the geographical effects in this subsection.
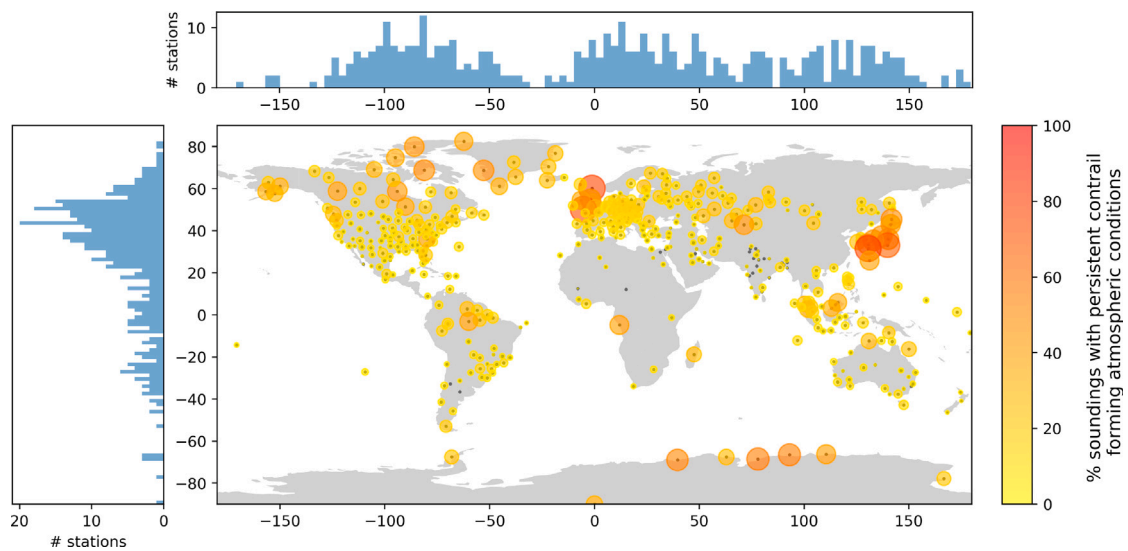
Fig. 6. Global distribution of persistent contrail-forming atmospheric conditions, with black dots indicating station locations, and shaded circles indicating the percent of soundings with atmospheric conditions satisfying persistent contrail formation. The vertical and horizontal histograms indicate the latitudinal and longitudinal distribution of IGRA stations.
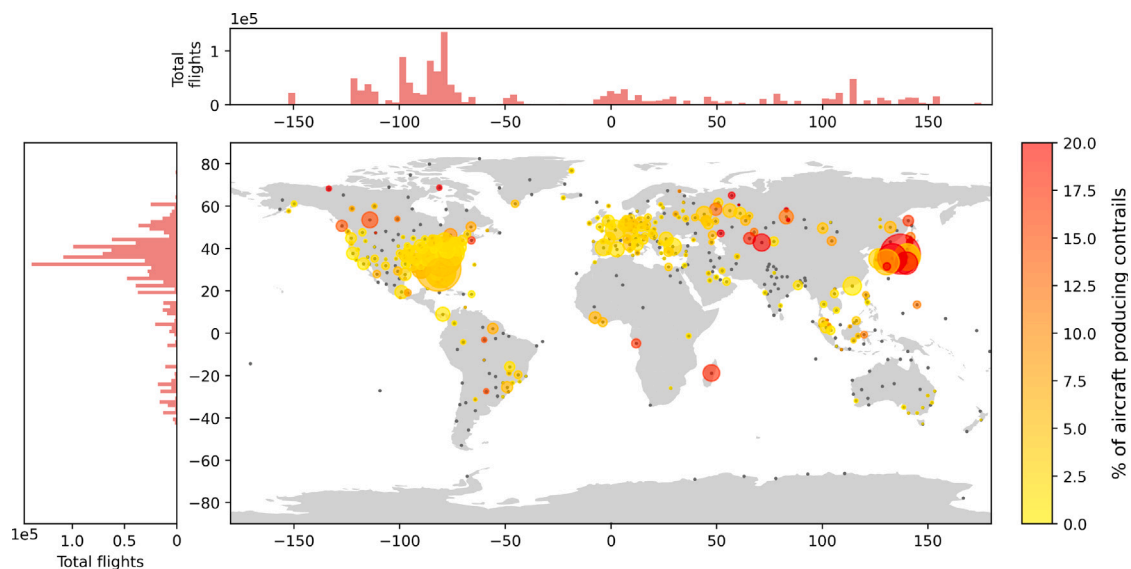

Fig. 7. Global distribution of aircraft producing persistent contrails, with black dots indicating station locations, and shaded circles indicating the percent of total aircraft and the size of the circle indicating the absolute number of aircraft. The vertical and horizontal histograms indicate the latitudinal and longitudinal distribution of total flights.

Fig. 6 shows a global yearly overview of the percent of weather balloon soundings that include persistent contrail-forming atmospheric conditions, namely instances of RH_i exceeding 100% and temperature falling below $-40°$ (233.15 K). The black dots indicate the locations of the stations, and the shade and size of the circles indicate the percentage of soundings when atmospheric conditions allow for the formation of persistent contrails. The vertical and horizontal histograms indicate the latitudinal and longitudinal distribution of IGRA stations.

Fig. 7 shows a similar graph, however here the colouring of the circles indicates the percentage of aircraft that fly through these atmospheric conditions that allow for persistent contrail formation. The sizes of the circles indicate the number of flights in absolute terms. The vertical and horizontal histograms display the latitudinal and longitudinal distribution of the total number of flights. Large and darker red circles mean that not only the percentage of contrail-forming flights is high, but also the absolute number of contrail-forming flights is high, as well.
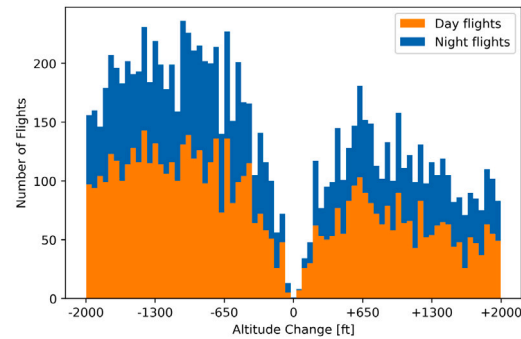
5.4. Flight level change

We previously illustrated the opportunity to change the flight level to stop contrail formation in Fig. 3. In Fig. 8.a, we show a histogram of the absolute nearest distance for a flight to *exit* a persistent contrail-forming atmospheric layer. From literature (Avila et al., 2019), we know that altitude changes of less than 2000 ft are feasible, and the histogram in Fig. 8.b shows that this accounts for a significant portion (31%) of the flights.

Filtering the histogram for deviations of less than 2000 ft, we show the absolute deviations in Fig. 8.b, with negative values indicating a decrease and positive values indicating an increase in the required altitude. A majority of 61% of the flights required an altitude decrease (an average of 1071 ft (326.44 m)), while the remaining 39% required an increase to exit the ISSR (an average of 996 ft (303.58 m)). We also indicate a distinction between day and night flights using colour in the histogram.
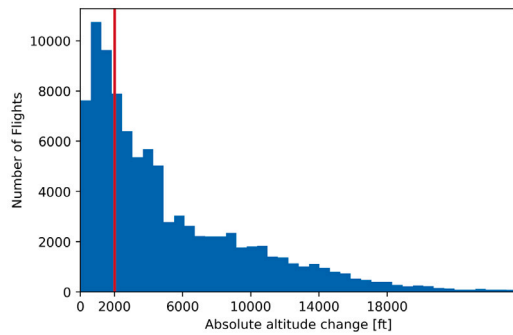
(a) Histogram of all flight level changes (absolute values), with the vertical red line at 2000 ft.

(b) Histogram of flight level changes, less than 2000 ft, with negative values indicating a decrease and positive values indicating an increase in altitude to avoid ISSRs.

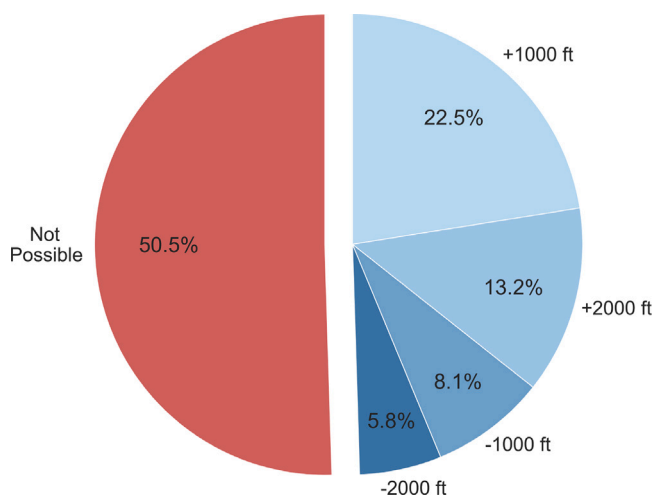**Fig. 8.** Flight level changes required to stop producing contrails.

Fig. 9. Pie chart of flight level changes, where only discrete altitude options are available, among range the four steps of 1000 ft. If no alternative altitude can be found, the flight was categorized as *not possible*. A total of 64,288 were considered.

In the current airspace configuration, custom altitude changes (as shown in Fig. 8.b) are not always possible. Typically, only discrete steps are available when requesting an altitude change. These alternative altitudes are shown in Fig. 9. For each contrail-forming flight, we first checked whether an altitude change of +1000 ft would prevent persistent contrail formation. If it is insufficient, we then considered a higher increase of +2000 ft. Conversely, we also examined the possibility of reducing the altitude by −1000 ft and −2000 ft as alternatives. This order was chosen as altitude decreases are unfavourable when minimizing climate impact since they decrease fuel efficiency (Avila et al., 2019; Schumann et al., 2011). If none of these alternative altitudes are possible, we categorized it as *not possible* in Fig. 9, which occurs in 50.5% of cases.

In Fig. 10, we show the global distribution of the occurrences requiring a flight level change of less than 2000 ft to stop contrail production. The shading of the circles indicates the percentage of total flights that are suitable for such an altitude change, and the size of the circle indicates the number of these flights.

5.5. Additional CO_2 emissions

Since flight emission estimations can be heavily influenced by the aircraft mass, we performed a sensitivity analysis by varying the initial mass between 75% and 100% of the maximum take-off weight to study

the additional CO_2 emissions caused by the altitude change. In Fig. 11, each line represents the additional emissions (in percent) in a month with different aircraft mass assumptions.

5.6. Climate impact

In this subsection, we demonstrate the true climate gains feasible through the altitude deviations described in Section 5.4. In Fig. 12, we show the top 25 stations where the largest climate gains can be made, with the smallest percentage of flights changing altitude. We limited the stations to those with a minimum of 10,000 yearly flights. Following the method described in Section 4.3, we determined the radiative forcing for all contrail-forming flights and then the radiative forcing for flights suitable for an altitude change of less than 2000 ft. The ratio between these two values, referred to as the percent of radiative forcing that can be prevented, is shown in Fig. 12.

5.7. Safety

We analyse the potential loss of separation and conflicts due to the change of flight altitude without any air traffic control coordination.

Table 1 shows the change in the number of actions required for intrusion prevention and for conflict solving, because of the change in altitude required to avoid contrail creation. The column *'change in number of intrusions'* refers to the scenario illustrated in Fig. 4.b, and *'change in number of conflicts'* refers to the one in Fig. 4.a. The total number of flights and the number of flights with a changed altitude (and their percentage of the total) are also shown.

It is important to highlight that within controlled airspace, addressing these additional conflicts requires only a minimal additional effort for air traffic controllers. Therefore, the safety risks associated with flight altitude changes to prevent contrail formations are nearly negligible.

Table 1 shows that there is only a slight increase in the number of intrusions or conflicts when changing altitudes for contrail prevention. This result is somewhat expected based on the small percentage of flights that required an altitude change for contrail prevention, and the relative emptiness of the airspace in general, even considering the large number of flights analysed for the year 2021 (2.6 million).

6. Discussion

In this section, we adhere to the general structure of the results section for discussion.
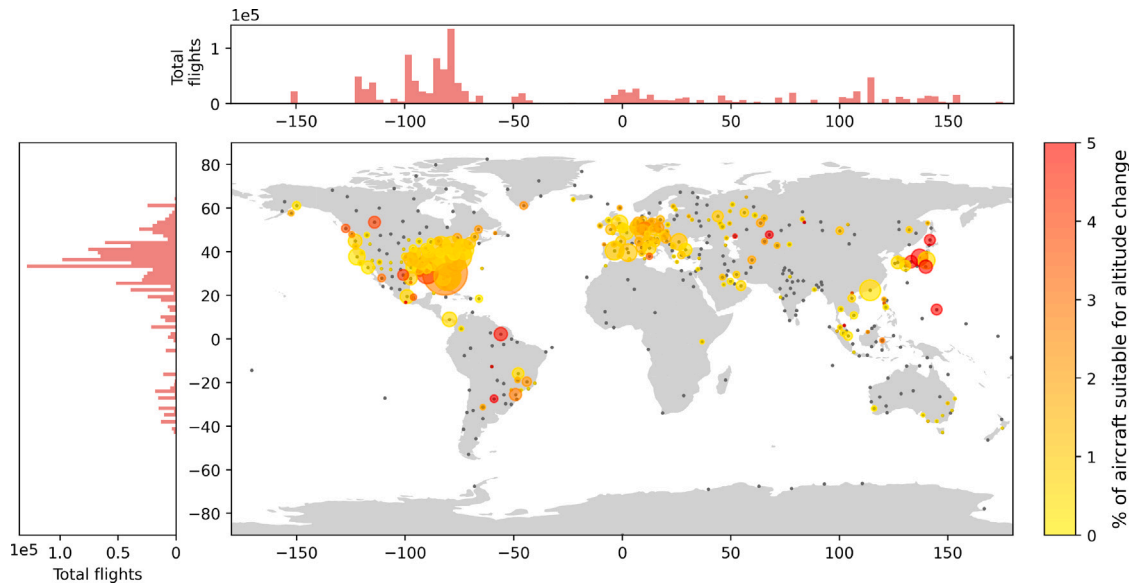
Fig. 10. Global distribution of the percent of aircraft where an altitude change of less than 2000 ft would prevent them from producing contrails. The size of the circles indicates the number of suitable flights. The vertical and horizontal histograms indicate the latitudinal and longitudinal distribution of all flights.
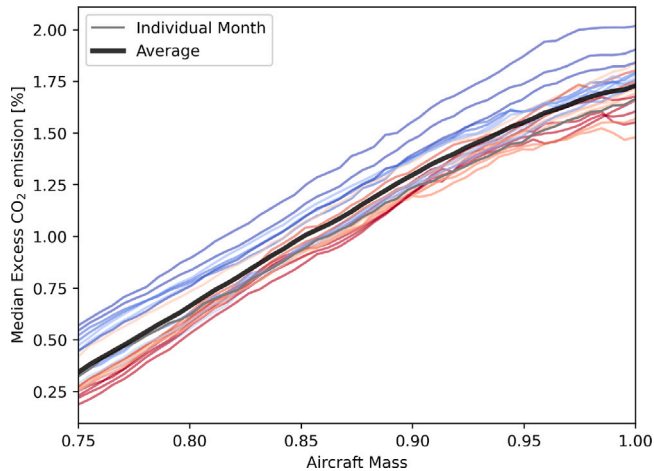

Fig. 11. Sensitivity analysis for additional CO_2 emissions, with varying initial mass. Each line represents a single month, and the black line shows the average of all 24 months. Seasonal dependency is also illustrated here, with colder winter months in blue colours and warmer summer months in red.

Table 1
Monthly actions for intrusion prevention and actions for conflict solving. The total number of flights and the number of flights with a changed altitude (and their percentage of the total) are also shown.

	Actions for intrusion prevention	Actions for conflict solving	Total flights	Flights with changed altitude
January	0	+1	166,651	1154 (0.93%)
February	0	0	149,998	1168 (0.78%)
March	0	0	191,979	1338 (0.70%)
April	+1	0	200,296	1452 (0.72%)
May	0	0	208,731	1604 (0.77%)
June	0	+1	220,712	1580 (0.71%)
July	0	0	243,836	1492 (0.61%)
August	+1	+2	238,265	1862 (0.78%)
September	0	0	227,643	2,340 (1.02%)
October	0	0	238,664	2,372 (0.99%)
November	+1	0	232,122	2,254 (0.97%)
December	+1	0	239,523	2,974 (1.24%)

6.1. Quantifying contrails

Based on atmospheric data from the same source as (Roosenbrand et al., 2022; Avila et al., 2019) estimates that 15% of flights generate contrails in the United States, while our results show 4.6%. Avila and Sherry (2019) indicates a maximum of 34% of flights generate contrails on a given day, with the daily average percentage of flights at 15.1% with a median of 13.8%. However, these results encompass the mid-Atlantic, where ISSRs are very prevalent and has a high air traffic volume.

OpenSky and IGRA both have limitations regarding coverage over oceans, and so could not be included in this research. The limited data coverage over oceans likely contributes to the differences in overall contrail percentages. Further extensive analysis using satellite networks (Cappaert, 2020) for cross-Atlantic flights should confirm this hypothesis.

6.2. Temporal effects

Teoh et al. (2022) reveals that while air traffic peaks in summer, persistent contrails are more common in winter. Fig. 5 supports this finding.

Notably, Avila et al. (2019) indicates that summer flights exhibit roughly three times higher Net Radiative Forcing than other months. Therefore, though fewer flights produce contrails in summer, their climate impact per flight is higher, especially given the greater number of flights in that season.

Fig. 5.b displays a reduction in aircraft suitable for altitude changes during winter, likely due to increased ISSR vertical extent (Hoinka et al., 1993).

The dominance of Northern Hemisphere seasonal cycle in the IGRA data influences the estimate of night flights, with an increase during winter and a decrease in summer. Weather balloon data skewed to the Northern Hemisphere shows a higher proportion of night flights compared to earlier studies (Stuber et al., 2006) (33.2% compared to literature 25%). However, night flights contribute disproportionately to contrail forcing (Stuber et al., 2006), suggesting the potential of flight rescheduling for climate impact mitigation.
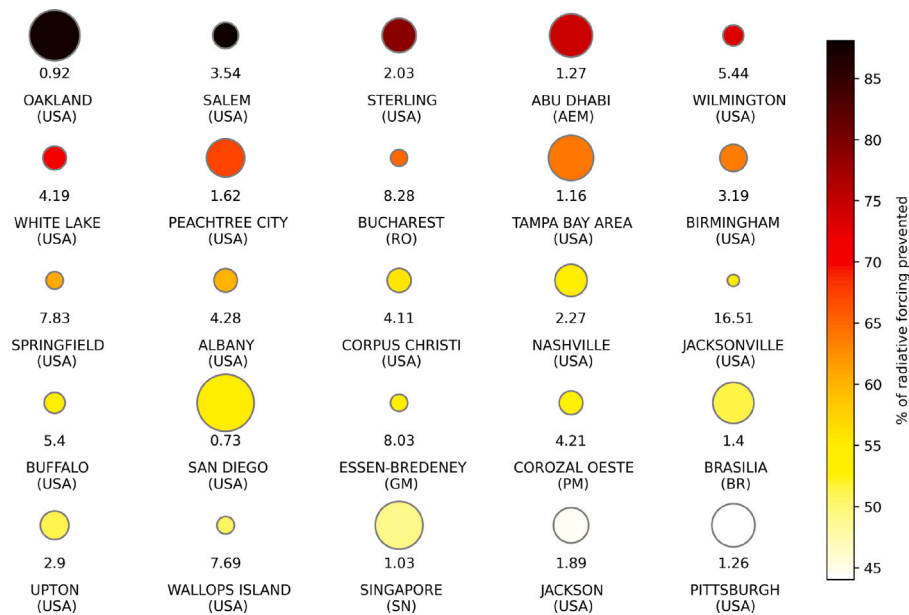
Fig. 12. Top 25 stations for minimizing contrail radiative forcing, with more than 10,000 yearly flights. The circle colour indicates the percent of contrails, which are prevented, and the size of the circle is correlated to the number of flights that need to be diverted (specifically the inverse). This percentage of flights is also shown below the circles. Thus, large circles in dark red indicate that with a few altitude diversions, a large percentage of contrails can be prevented.

6.3. Geographical effects

Avila et al. (2019) focuses on contrail generation in the contiguous United States and notes greater prevalence in the southeastern states. Our results (Fig. 7) align with this observation, but underestimate contrail formation in the Pacific region of the U.S.A. (Roosenbrand et al., 2022). These discrepancies may stem from contrail-forming regions mainly over the ocean, not covered by IGRA ground stations. Linking IGRA to ECMWF data in these oceanic regions may offer a solution.

Meyer et al. (2007) notes contrail prevalence in Southern and Eastern Asia, corroborated by our analysis (Fig. 6). With the region's increasing air traffic, contrail mitigation becomes increasingly relevant.

In Europe, a high volume of flights, rather than a high percentage of contrail-producing flights, drives contrail prevalence. However, atmospheric conditions allowing contrail formation are relatively frequent (Fig. 6). Further research is needed to understand altitude adjustments' impact on contrail formation.

6.4. Flight level change and its policy implications

Due to the discrete points used for the measurements and not using interpolation, the required altitude change could be overestimated, and might be even less in reality.

In our analysis, the aircraft has the option to either increase or decrease the altitude to *exit* the atmospheric layer. In Fig. 8, we see that in a majority (63%) of these flight alterations, the nearest option is reached by decreasing the altitude. Altitude decreases are generally unfavourable for minimizing climate impact due to decreased fuel efficiency (Avila et al., 2019; Schumann et al., 2011). Additional research on the trade-off between contrail climate effects and fuel burn is necessary.

A crucial result of this paper can be seen in Fig. 9: nearly 50% of contrail-forming flights can be mitigated through discrete altitude changes within the range of −2000 ft, −1000 ft, +1000 ft, and +2000 ft, already common in air traffic management.

Fig. 10 highlights regions where contrails could be minimized within current aircraft operations: mid-Western Europe, southeastern United States, and Southeast Asia.

6.5. Additional CO_2 emissions

Altitude diversions result in 0.25% to 2.0% additional carbon emissions, depending on aircraft mass assumptions. This range aligns with existing literature (<1% additional fuel burn - (Avila et al., 2019); 2.24% fuel - (Sridhar et al., 2010)).

The vertical extent of ISSRs in winter requires larger altitude deviations (Hoinka et al., 1993), resulting in higher CO_2 emissions, as depicted in Fig. 11 (bluish hues for winter and red for summer). Avila et al. (2019) points out that in the Summer months, more flights require an altitude *increase* to avoid ISSR's, which would also explain the lower fuel burn required we see.

With comparable results (Avila et al., 2019), concludes that the additional fuel burn caused by the altitude change from the original to the new flight level is *not* statistically significant. Mainly because the additional fuel burn was compensated by the advantage of cruising at higher altitudes with lower drag.

7. Conclusion

Global contrail formation was assessed using OpenSky, Spire, and weather balloon data from the years 2021 and 2022. Furthermore, the magnitude of altitude changes necessary to minimize contrail formation was quantified. The analysis of these persistent contrail flights shows that there are strong geographical and seasonal influences for identifying contrail-forming flights.

The key aspects examined in this study, namely safety, discrete altitude steps, and additional CO_2 emissions, are often cited as reasons that make altitude deviations for contrail prevention impractical. However, through a thorough analysis conducted within the scope of our research, we have effectively addressed and refuted these arguments. Of the required altitude changes to avoid contrails, 50.5% are possible within the discrete altitude step and a maximum of 2000 ft.

By carefully dissecting these concerns, we have demonstrated that the perceived obstacles surrounding safety, discrete altitude steps, and additional CO_2 emissions can be overcome. This research has successfully disarmed these commonly presented arguments against the feasibility of altitude deviations as a practical approach for contrail formation prevention, as well as illustrating the substantial climate gains possible through this approach.

CRediT authorship contribution statement

Esther Roosenbrand: Conceptualization, Methodology, Writing – original draft, Data curation, Writing – review & editing, Visualization, Software. **Junzi Sun:** Conceptualization, Methodology, Writing – original draft, Writing – review & editing, Visualization, Software. **Jacco Hoekstra:** Conceptualization, Methodology, Writing – review & editing.

Declaration of competing interest

The authors declare that they have no known competing financial interests or personal relationships that could have appeared to influence the work reported in this paper.

Data availability

Open and public data are used for this paper.

References

Agarwal, A., Meijer, V., Eastham, S., Speth, R., Barrett, S., 2022. Reanalysis-driven simulations may overestimate persistent contrail formation by 100-250%. Environ. Res. Lett. 17.

Avila, D., Sherry, L., 2019. A contrail inventory of U.S. airspace (2015). In: Proceedings IEEE Integrated Communications, Navigation and Surveillance (I-CNS) Conference 2019, Vol. 9.

Avila, D., Sherry, L., Thompson, T., 2019. Reducing global warming by airline contrail avoidance: A case study of annual benefits for the contiguous united states. Transp. Res. Interdiscipl. Perspect. 2.

Baneshi, F., Soler, M., Simorgh, A., 2023. Conflict assessment and resolution of climate-optimal aircraft trajectories at network scale. Transp. Res. Part D: Transp. Environ. 115, 103592.

Buehler, S., Courcoux, N., 2003. The impact of temperature errors on perceived humidity supersaturation. Geophys. Res. Lett. 30.

Cappaert, J., 2020. The spire small satellite network. In: Handbook of Small Satellites: Technology, Design, Manufacture, Applications, Economics and Regulation. pp. 1–21.

Corti, T., Peter, T., 2009. A simple model for cloud radiative forcing. Atmos. Chem. Phys. 9, 5751–5758.

Dirksen, R.J., Sommer, M., Immler, F.J., Hurst, D.F., Kivi, R., Vömel, H., 2014. Reference quality upper-air measurements: Gruan data processing for the vaisala rs92 radiosonde. Atmos. Meas. Tech. 7, 4463–4490.

Durre, I., Vose, R., Wuertz, D., 2021. Overview of the integrated global radiosonde archive. Atmos. Environ. 244.

Durre, I., Yin, X., Vose, R., Applequist, S., Arnfield, J., 2018. Enhancing the data coverage in the integrated global radiosonde archive. J. Atmos. Ocean. Technol. 35.

Ferris, P., 2007. The formation and forecasting of condensation trails behind modern aircraft. Meteorol. Appl. 3.

Gao, H., Hansman, R., 2013. Aircraft Cruise Phase Altitude Optimization Considering Contrail Avoidance (Master's Thesis). Department of Aeronautics, Massachusetts Institute of Technology.Report No. ICAT-2013-10.

Grewe, V., Dahlmann, K., Flink, J., Frömming, R., Gierens, K., Heller, R., Hendricks, J., Jöckel, P., Kaufmann, S., et al., 2017. Mitigating the climate impact from aviation: Achievements and results of the dlr wecare project. Aerospace 4 (34).

Hoinka, K.P., Reinhardt, M.E., Metz, W., 1993. North atlantic air traffic within the lower stratosphere: Cruising times and corresponding emissions. J. Geophys. Res.: Atmos. 98, 23113–23131.

Karcher, B., 2018. Formation and radiative forcing of contrail cirrus. Nat. Commun. 9.

Lee, D., 2021. The contribution of global aviation to anthropogenic climate forcing for 2000 to 2018. Atmos. Environ. 244.

Lee, D., Pitari, G., Grewe, V., Gierens, K., Penner, J., Petzold, A., Prather, M., Schumann, U., Bais, A., Berntsen, T., Iachetti, D., Lim, L., Sausen, R., 2010. Transport impacts on atmosphere and climate: Aviation. Atmos. Environ. 44, 4678–4734.

Meyer, R., Buell, R., Leiter, C., Mannstein, H., Pechtl, S., Oki, T., Wendling, P., 2007. Contrail observations over southern and eastern asia in noaa/avhrr data and comparisons to contrail simulations in a gcm. Int. J. Remote Sens. 28, 2049–2069.

Miloshevich, L.M., Vömel, H., Whiteman, D.N., Leblanc, T., 2009. Accuracy assessment and correction of vaisala rs92 radiosonde water vapor measurements. J. Geophys. Res.: Atmos. 114.

Moradi, I., Buehler, S.A., John, V.O., Eliasson, S., 2010. Comparing upper tropospheric humidity data from microwave satellite instruments and tropical radiosondes. J. Geophys. Res.: Atmos. 115.

Organization, I.C.A., 2016. Doc 4444: Procedures for air navigation. Air Traffic Manag. 16.

Ramaswamy, V., Boucher, O., Haigh, J., Hauglustaine, D., Haywood, J., Myhre, G., et al., 2001. Radiative Forcing of Climate Change. Cambridge Univ. Press, Cambridge.

Roosenbrand, E., Sun, J., Hoekstra, J., 2022. Examining Contrail Formation Models with Open Flight and Remote Sensing Data. SESAR Innovation Days 2022.

Rosenow, J., Fricke, H., 2019. Individual condensation trails in aircraft trajectory optimization. Sustainability 11.

Sanz-Morère I. Eastham, S.D., Allroggen, F., Speth, R.L., Barrett, S.R., 2021. Impacts of multi-layer overlap on contrail radiative forcing. Atmos. Chem. Phys. 21, 1649–1681.

Sanz-Morère I. Eastham, S.D., Speth, R.L., Barrett, S.R., 2020. Reducing uncertainty in contrail radiative forcing resulting from uncertainty in ice crystal properties. Environ. Sci. Technol. Lett. 7, 371–375.

Sausen, R., Hofer, S., Gierens, K., Bugliaro, L., Ehrmanntraut, R., Sitova, I., Walczak, K., Burridge-Diesing, A., Bowman, M., Miller, N., 2023. Can we successfully avoid persistent contrails by small altitude adjustments of flights in the real world? Meteorol. Z..

Schumann, U., 1996. On conditions for contrial formation from aircraft exhausts. Meteorol. Z. 4-23.

Schumann, U., 2005. Formation, properties and climatic effects of contrails. Physique 6, 549–565.

Schumann, U., Graf, K., Mannstein, H., 2011. Potential to reduce the climate impact of aviation by flight level changes. p. 3376.

Service, A.W., 1981. Forecasting aircraft condensation trails. ADA111876.

Simorgh, A., Soler, M., González-Arribas, D., Linke, F., Lührs, B., Meuser, M.M., Dietmüller, S., Matthes, S., Yamashita, H., Yin, F., Castino, F., Grewe, V., Baumann, S., 2023. Robust 4d climate-optimal flight planning in structured airspace using parallelized simulation on gpus: Roost v1.0. Geosci. Model Dev. 16, 3723–3748.

Simorgh, A., Soler, M., González-Arribas, D., Matthes, S., Grewe, V., Dietmüller, S., Baumann, S., Yamashita, H., Yin, F., Castino, F., Linke, F., Lührs, B., Meuser, M.M., 2022. A comprehensive survey on climate optimal aircraft trajectory planning. Aerospace 9.

Soden, B.J., Lanzante, J.R., 1996. An assessment of satellite and radiosonde climatologies of upper-tropospheric water vapor. J. Clim. 9, 1235–1250.

Sonntag, D., 1994. Advancements in the field of hygrometry. Meteorol. Z. 3.

Sridhar, B., Chen, N., Ng, H., 2010. Fuel efficient strategies for reducing contrail formations in United States airspace. In: AIAA/IEEE Digital Avionics Systems Conference - Proceedings.

Sridhar, B., Ng, H., Linke, F., Chen, N., 2014. Benefits analysis of wind-optimal operations for trans-atlantic flights. In: 14th AIAA Aviation Technology, Integration, and Operations Conference.

Strohmeier, M., Xavier, O., Jannis, L., Schäfer, M., Lenders, V., 2021. Crowdsourced air traffic data from the opensky network 2019–2020. J. Air Transp. Manag. 94.

Stuber, N., Forster, P., Radel, G., 2006. The importance of the diurnal and annual cycle of air traffic for contrail radiative forcing. Nature 441, 864–867.

Sun, J., Hoekstra, J.M., Ellerbroek, J., 2020. Openap: An open-source aircraft performance model for air transportation studies and simulations. Aerospace 7.

Teoh, R., Schumann, U., Gryspeerdt, E., Shapiro, M., Molloy, J., et al., 2022. Aviation contrail climate effects in the North Atlantic from 2016 to 2021. Atmos. Chem. Phys. 22.

Trenberth, Kevin E, Fasullo, John T, Kiehl, Jeffrey, 2009. Earth's global energy budget. Bulletin of the american meteorological society 90 (3), 311–324.